Petrology, geochemistry (Isotopic geochemistry)

Fluid generation in the Boucheville Basin as a consequence of the North Pyrenean metamorphism

Philippe Boulvais

Université de Rennes-1, OSUR-Geosciences, UMR CNRS 6118, campus de Beaulieu, 35042 Rennes cedex, France

ABSTRACT

Metamorphic fluids transport heat and matter. In the Boucheville Basin (North Pyrenean Zone), the circulation of metamorphic fluids is attested by abundant synmetamorphic quartz – calcite veins. The Boucheville Basin formed during the Albian extensional regime and was filled by the so-called "Albian flysch". The basin underwent a thermal overprint (the North Pyrenean Metamorphism) related to the exhumation of nearby mantle rocks that advected large amounts of heat to the upper crustal levels. The oxygen and carbon isotope compositions of quartz – calcite veins and their host rocks show strong buffering of the composition of the fluids by the Albian metamorphic host rocks. Some host rocks are depleted in calcite near vein contacts showing that some of the elements implicated in crystal growth in veins were derived from the local host rock. The Albian rocks display a range of oxygen and carbon isotope compositions potentially related to closed-system processes of decarbonation–dehydration. We argue then that the fluids that circulated throughout the Boucheville Basin were generated within the basin itself. Their upward migration led to heat advection in the metamorphic pile, a consequence of which was some homogenization of the recrystallization temperatures in the basin.

© 2015 Académie des sciences. Published by Elsevier Masson SAS. This is an open access article under the CC BY-NC-ND license (http://creativecommons.org/licenses/by-nc-nd/4.0/).

1. Introduction

Veins represent the locus of fluid circulation. In open-system conditions, fluids are generated at distance, outside the studied geological system, and flow towards the site of vein formation. In closed-system conditions, fluids are generated locally and allow redistribution of matter to produce veins. In the former case, heat and matter can be transported over large distances (the system is "open") whereas in the latter only small-scale redistribution of matter is permitted (the system is "closed").

In the North Pyrenees, HT-LP metamorphism affected an east–west-elongated zone, in close association with the North Pyrenean Fault (FNP; Fig. 1a). This zone is known as the North Pyrenean Metamorphic Zone (NPMZ). Recently, Clerc et al. (2015) have associated this thermal anomaly with extreme thinning of the Pyrenean paleo-margins in mid-Cretaceous times, prior to the Pyrenean collision (Upper Cretaceous – Eocene). In a comprehensive petrological and geochemical study of the sediments affected by the North Pyrenean Metamorphism (NPM), Ravier (1959) described isochemical recrystallization during metamorphism, which could correspond to a "closed-system" evolution. In contrast, Dauteuil and Ricou (1989) proposed that fluids may have acted to transfer heat regionally, which corresponds to "open-system" conditions.

In this study, we focus on the Boucheville Basin (Fig. 1b), filled with Albian quartz (silty)-calcareous black shales (Albian flysch deposits; e.g., Souquet et al., 1985), which recorded temperatures up to 580 °C during the NPM (Chelalou et al., this issue). Numerous veins occur in the

black shales and may thus provide information on the nature of the fluid-rock interaction system ("closed" vs "open") prevailing during metamorphism. We use the oxygen, carbon and strontium isotope signatures of both veins and host black shales to show that veins formed without the involvement of externally derived fluids. We thus describe a "closed-system" evolution in which a significant proportion of the elements forming mineral in veins come from the local host rocks.

2. Geological context

The North Pyrenean Metamorphic Zone (NPMZ) is a narrow zone located immediately north of the North Pyrenean Fault (NPF; Fig. 1a). This fault limits the axial zone from the NPMZ. The exact nature of this structure remains unclear in the context of the extreme thinning of the Pyrenean paleo-margin during the eastward movement of Iberia relative to Europe during Albian times (Choukroune, 1992; Choukroune et al., 1973; Olivet, 1996). Close to the NPF, on its northern side over a length of about 150 km, forty lherzolitic bodies of variable size are reported (Fabriès et al., 1998; Monchoux, 1970). A mid-Cretaceous crustal emplacement age of these bodies has been proposed (105–110 Ma; Henry et al., 1998). Serpentinization of peridotites and development of ophicalcites are abundant (Clerc et al., 2014). Locally, discrete eruptive and plutonic bodies of alkaline affinity were emplaced in the area, especially in the central and western Pyrenees (Montigny et al., 1986). During the Albian period again, intense hydrothermal activity is evidenced throughout the area by 1) numerous talc/chlorite ore deposits (Boulvais et al., 2006; Moine et al., 1989) with a mineralization age of 112–97 Ma (Schärer et al., 1999) and 2) albitization and sodic-calcic metasomatism of rocks of variable nature with ages ranging from 117 to 92 Ma (Boulvais et al., 2007; Fallourd et al., 2014; Poujol et al., 2010).

Particularly well exposed in the NPMZ are quartz – calcareous black shales of Albian age, deposited in basins north of the NPF including the Boucheville Basin (Fig. 1b). The initial geometry of the basins in the Albian is described in detail by Clerc and Lagabrielle (2014) and Chelalou et al. (this issue). Inversion of the basins caused by northward motion of Iberia began during the Upper Cretaceous (Choukroune, 1976). The Albian black shales have been variably metamorphosed up to HT-LP metamorphic conditions (3 kbar–4 kbar; 500 °C–600 °C; Golberg and Leyreloup, 1990). Ages ranging from 98 Ma to 87 Ma (Cenomanian – Turonian) have been obtained by Ar–Ar dating on minerals separates from Mesozoic metasediments (Albarède and Michard-Vitrac, 1978; Golberg and Maluski, 1988). The recent synthesis of Clerc et al. (2015) highlights the east-west thermal zonation within the NPMZ, the maximum thermal conditions being encountered in the east part. In the Boucheville Basin, Chelalou et al. (this issue) report temperatures between 530 °C and 580 °C, with a homogeneous distribution throughout the basin. Unmetamorphosed equivalents of the Albian metamorphic rocks from the Boucheville Basin occur a few kilometres further north, in the Saint-Paul-de-Fenouillet and Bas-Agly Basins.

3. Petrography of the Albian rocks

Samples from the Boucheville Basin have been collected in transects along road outcrops named CARY, DSX, SOU, VIR and BOUZ (Fig. 1b). For comparison, samples of both Albian metamorphic rocks (TAU) and unmetamorphosed Albian shales (AXAT and CDF) have been collected to the west and to the north of the Boucheville Basin (Fig. 1), respectively. Numerous calcite veins with large euhedral crystals formed in association with Late Cretaceous–Eocene reverse faulting are not considered in this study.

The unmetamorphosed Albian sediments are quartz (silty) – calcareous black shales. They are comprised, in variable amounts, of calcite, quartz, clays (chlorite and sericite have been identified by X-Ray diffraction; Ravier, 1959) and organic matter. In Fig. 2, their heterogeneity is highlighted by the large range in CaO and CO_2 contents, which can be interpreted by mixing between calcite and a silicate detrital phase. The mineralogical and geochemical heterogeneity of the Albian sediments is also observed in their metamorphic counterparts (Fig. 2); the metamorphic rocks have lower CO_2 contents for a given CaO content. This is likely related to the release of CO_2 through decarbonation reactions during metamorphism. The Albian metamorphic rocks comprise variable amounts of Cal, Qtz (from 10% to 50%), An-rich plagioclase (Pl) (from 0% to 45%), biotite (Bt) (from 0% to 15%), graphite (Gr), minor amounts of tourmaline, sulphides and titanite. Scapolite is present in calcite-rich marble layers.

The veins are composed of calcite and quartz, in variable amounts (Table 1). The length of veins ranges from 1 m to 10 m and their width from 0.5 cm to 10 cm. They are generally deformed, folded (Fig. 3a) and/or transposed parallel to the foliation; none cross-cuts foliation at high angle. Foliation is sometimes visible in veins (Fig. 3b). Taken together, all this information shows that veins formed early during the deformation history of the basin, this deformation being associated with lithospheric stretching during mid-Cretaceous times (Clerc et al., 2015). The calcite content of veins seems related to the calcite content of the local host rocks: for example, the veins with the lowest calcite content (samples SOU 01-160a and SOU 01-163a) are hosted in rocks with a very low content of Cal, lower than 20 wt% (Table 1). In host rocks, a selvage is commonly observed at the contact with veins (Fig. 3c), which corresponds to a decrease in the calcite content. Biotite and sulphides sometimes develop in veins (Fig. 3c), in which case these minerals are also present in significant amounts in the host rock. From their structure and mineralogy, we can infer that the veins developed early in the regional deformation event and at elevated temperatures, sufficient to crystallize biotite, in relation to the NPM. This conclusion was also reached by Ravier (1959) and Choukroune (1976).

4. Analytical techniques

The O and C isotope compositions were measured using a VG SIRA 10 triple collector mass spectrometer at the University of Rennes-1, on the CO_2 released during the reaction of calcite with anhydrous H_3PO_4 at 25 °C (McCrea,
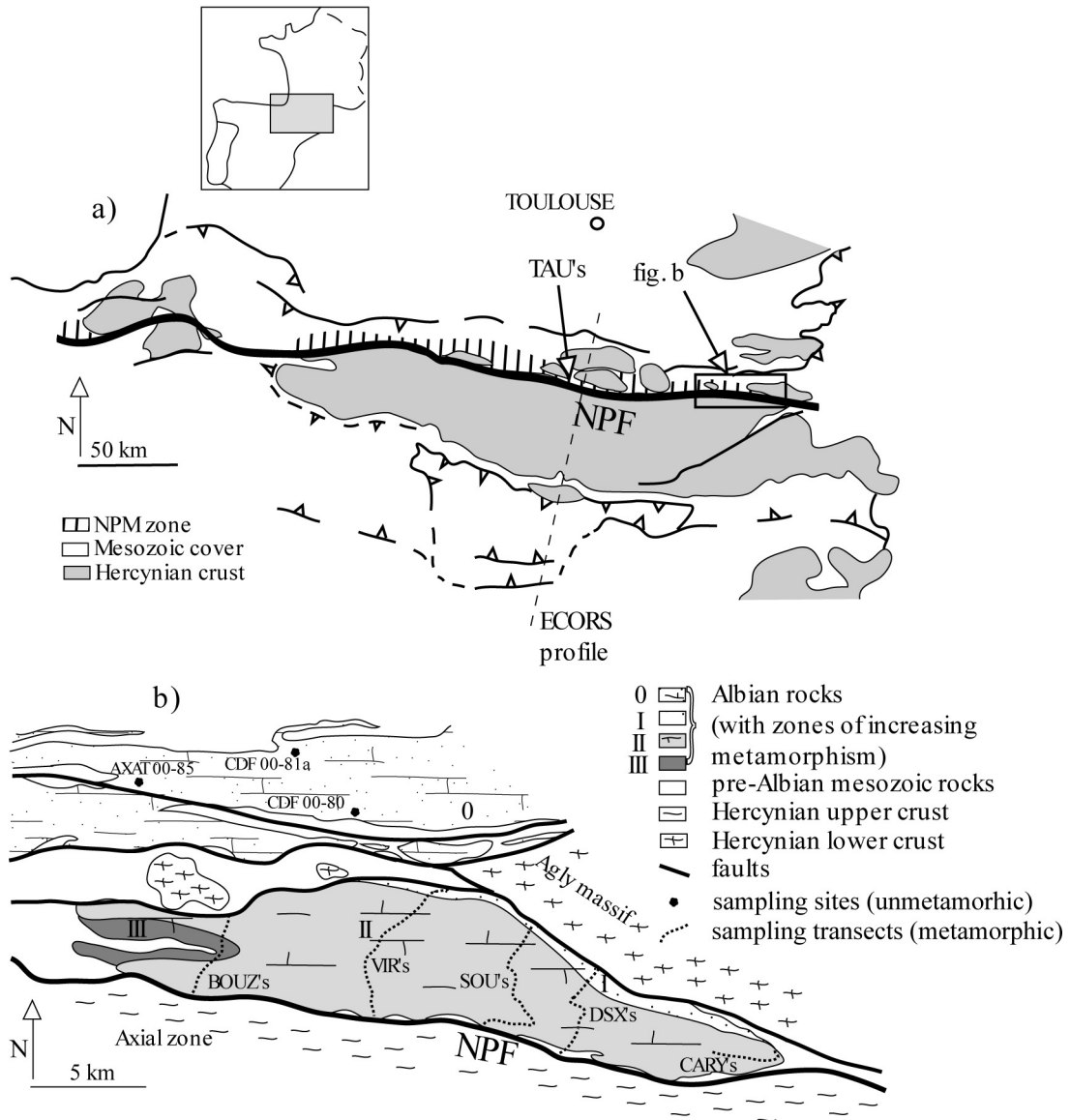
Fig. 1. (Colour online.) (**a**) Schematic map of the Pyrenees. The North Pyrenean Metamorphic Zone (NPMZ) is indicated by the vertical hatched zone immediately north of the North Pyrenean Fault (NPF). The location of the ECORS seismic profile is shown (Roure et al., 1989). TAU refers to the area of three metamorphic samples of Albian age used for comparison. (**b**) Geological map of the Boucheville Basin, showing the repartition of Albian rocks affected by different degrees of metamorphic recrystallization (after Ravier, 1959). Sampling traverses are labelled as the dashed lines. The location of three samples coming from the unmetamorphic zone (samples AXAT and CDF) is also indicated.

1950). The calcite content was calculated by measuring with an Hg manometer the amount of CO_2 released. The absolute precision of calcite content estimate is $\pm 5\%$. When sulphides are present in samples, the H_2S liberated during reaction was removed by reaction with Ag_3PO_4 at around 50 °C for 5 min by forming silver sulphate. For the oxygen isotope analysis of the silicate fraction of veins and black shales, the carbonate fraction was removed through leaching with 0.15 N HCl for 3 h. Oxygen was then extracted from the residual silicate fraction following the method of Clayton and Mayeda (1963). BrF_5 was used as an oxidising agent. NBS 19 (limestone), NBS 28 (Qtz) and internal-lab

standard references materials were continuously measured during the course of this work. NBS 19 measured values ($n = 12$) were $\delta^{18}O = 28.70 \pm 0.11‰$ (vs SMOW) and $\delta^{13}C = 1.91 \pm 0.06‰$ (vs PDB). No correction was added to carbonate results. NBS 28 value was $\delta^{18}O = 9.21 \pm 0.09‰$ ($n = 4$). A correction was therefore made accordingly on the oxygen composition of silicates. Replicate analyses of materials gave a reproducibility better than 0.1‰ for both oxygen and carbon isotope composition of carbonates and of about 0.2‰ for oxygen of silicates. Strontium analyses were performed on the soluble fraction of rocks, which is presumed to represent carbonate, in 0.15 N HCl for 1 h. Sr
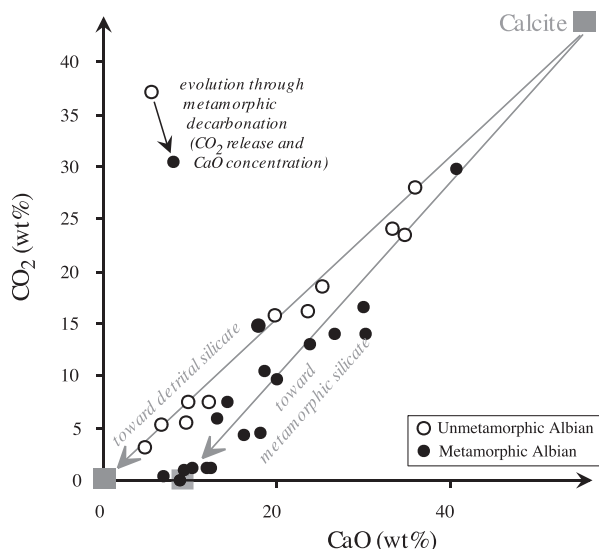
Fig. 2. CO_2 vs CaO variation diagram of Albian sediments and their metamorphosed equivalents (data from Ravier, 1959). The effect of decarbonation, i.e. CO_2 release and subsequent CaO enrichment by passive concentration is indicated by the arrow in the upper left corner. See text for details.

isotope ratios were measured on a Finnigan MAT 262 mass spectrometer at the University of Rennes-1. $^{87}Sr/^{86}Sr$ ratios were normalised to $^{86}Sr/^{88}Sr = 0.1194$. NBS 987 is used as a routine standard and give a long-term value of $^{87}Sr/^{86}Sr = 0.710250$. The Sr blank was 30 pg and was considered negligible.

5. Results

The O, C and Sr isotope compositions of Albian black shales and veins are reported in Table 1. The Albian metamorphic rocks of the Boucheville Basin show a limited range of $\delta^{18}O_{Cal}$ values from 25 to 21‰ and a more wide range of $\delta^{13}C$ from +3‰ to −6‰ (Fig. 4a), whereas unmetamorphosed Albian rocks have $\delta^{18}O_{Cal}$ values between 23.6‰ and 25.9‰ and $\delta^{13}C$ values between 0.6‰ and 1.5‰, values equal to or higher than their metamorphic equivalents (Fig. 4a). Samples TAU are undistinguishable from the samples from the Boucheville Basin. Both $\delta^{18}O_{Cal}$ and $\delta^{13}C$ of metamorphic rocks show a good correlation with the weight amount of calcite (Fig. 4b). In the Albian metamorphic rocks, the calcite fraction has a higher $\delta^{18}O$ value than the silicate fraction by about 1‰ to 1.5‰. Using the descriptions of Ravier (1959) we have estimated a mean modal composition for this silicate fraction in the Albian metamorphic rocks: 50% Qtz, 10% Bt and 40% Pl (bytownite). The theoretical equilibrium curves between calcite and such a silicate component are given in Fig. 5, using the fractionation factors of Zheng (1993a,b). We see that the calcite and the silicate phase of the Albian metamorphic rocks are in isotopic equilibrium at temperatures about 200 °C–300 °C. The Albian unmetamorphosed black shales consistently plot well below the curves.

The veins display a covariation of $\delta^{18}O$ and $\delta^{13}C$ that mimics the Albian metamorphic host rocks (Fig. 4a), veins having lower $\delta^{18}O_{Cal}$ ($\Delta^{18}O_{vein–HR(mean)} = −0.3‰$; Fig. 6a) and higher $\delta^{13}C$ ($\Delta^{13}C_{vein–HR(mean)} = +1.5‰$; Fig. 6b) than their host rock. In veins, calcite has lower $\delta^{18}O$ values than quartz by about 1.5‰. This fractionation is consistent with isotopic equilibrium between calcite and quartz at temperatures of about 200 °C–300 °C (Fig. 5).

At a small-scale contact where the calcite content decreases toward the vein, $\delta^{18}O_{Cal}$ and $\delta^{13}C$ values vary significantly towards the vein (Fig. 7b,c). Interestingly, $\delta^{18}O_{Cal}$ values increase in that direction, whereas the vein has a lower value than the host rock and $\delta^{13}C$ values decrease, whereas the vein has a higher value than the host rock. None of these variations can result therefore from a simple diffusional exchange between the vein and the host rock.

The Sr isotope compositions of calcite from four veins-host rock pairs are reported in Table 1 and in Fig. 8 together with the weight amount of calcite. Two of the host rocks are biotite-rich whereas the two are biotite-poor. The Albian metamorphic rocks have $(^{87}Sr/^{86}Sr)_{Cal}$ ratios between 0.7074 in biotite-poor and calcite-rich samples and 0.7094 in biotite-rich and calcite-poor ones. The lowest value is identical to that of mid-Cretaceous seawater ($^{87}Sr/^{86}Sr = 0.7074$; Veizer, 1989). As a rule, veins have lower $(^{87}Sr/^{86}Sr)_{Cal}$ ratios than their host rock, the difference being more important in biotite-rich and calcite-poor host rocks. Along the SOU 01-160 profile (Fig. 7d), the $(^{87}Sr/^{86}Sr)_{Cal}$ ratio increases slightly in the host rock towards the vein, from 0.70944 to 0.70985.

6. Discussion

6.1. Open vs closed-system

The stable isotopic tool can allow us to characterize fluid regimes in terms of "open" vs "closed" system evolution. In an "open-system regime", the circulation of large amounts of externally-derived fluids allows them to preserve their original signature during interaction with rocks. Veins formed under such regime acquire homogeneous isotopic compositions, which differ to those of the fluid only because of the fluid-vein isotopic fractionation. In a "closed-system" regime, the isotopic compositions of the fluids are buffered by those of the rocks with which they interacted. Veins formed that way thus acquire heterogeneous isotopic compositions which mimic the heterogeneity of their host rock.

The Albian sedimentary protolith of the metamorphic rocks of the Boucheville Basin are mineralogically and geochemically heterogeneous (Fig. 2). The isotopic similarity between the studied Albian unmetamorphosed rocks and other comparable Albian sediments in western Europe ($\delta^{18}O = 25‰$ to 29‰, $\delta^{13}C = 0.5‰$ to 3‰; Grötsch et al., 1998; Nederbragta et al., 1998; Weissert and Bréhéret, 1991) argues for a limited role of diagenesis in the studied area. Variable calcite/quartz/clays ratios induced variable behaviour during metamorphic recrystallization. Metamorphic reaction progress is limited by the abundance of

Table 1

Mineralogical and isotopic compositions of Albian rocks and veins.

Sample	Location	Type	Mineralogy		Calcite				Silicate
			Biotite	Opaques	wt%	$\delta^{18}O$‰	$\delta^{13}C$‰	$^{87}Sr/^{86}Sr$	$\delta^{18}O$‰
CDF 00-80	1	Unmetamorphic Albian			24	24.0	0.59		21.8
CDF 00-81	2	Unmetamorphic Albian			98	25.9	1.45		
AXAT 00-85	3	Unmetamorphic Albian			24	23.6	1.43		21.8
CARY 00-72	1	Metamorphic Albian (II)	+	+	62	24.1	1.58		
CARY 00-73	2	Metamorphic Albian (II)	−	tr	97	24.8	1.23		
CARY 00-78	3	Metamorphic Albian (II)	++	+	51	22.1	2.53		
CARY 00-79	4	Metamorphic Albian (II)	+	+	23	21.4	1.05		
DSX 00-44	4	Metamorphic Albian (II)	+	++	34	22.5	0.92		
DSX 00-47	3	Metamorphic Albian (II)	+	+	54	22.9	0.84		
DSX 00-51a*	2	Vein, 1 to 3 cm wide			100	21.9	0.79		
DSX 00-51b*	2	Metamorphic Albian (I), 10 cm from 00-51a			55	22.4	0.46		
DSX 00-53	2	Metamorphic Albian (I)	tr	+	52	23.5	1.34		
DSX 00-57	1	Metamorphic Albian (I)	++	++	51	22.3	2.27		
DSX 00-58	1	Metamorphic Albian (I)	tr	++	45	22.1	1.40		
DSX 00-63	5	Metamorphic Albian (II), 20 cm from 00-62			22	22.9	−1.08		
DSX 00-64	5	Metamorphic Albian (II)			42	21.6	−1.50		
DSX 00-65	5	Metamorphic Albian (II)			40	21.4	−0.81		
DSX 00-66	6	Metamorphic Albian (II), 2 m from 00-67b's			34	22.2	0.79		
DSX 00-67b5	6	Metamorphic Albian element in breccia			37	21.6	−5.43		
DSX 00-68	7	Metamorphic Albian (II)			51	22.6	0.49		
SOU 01-145	1	Metamorphic Albian (II)	+++	+	51	21.8	1.96		
SOU 01-149a*	3	Vein, 2 cm wide	+	tr	91	21.5	2.96		23.2
SOU 01-149b*	3	Metamorphic Albian (II), 2 ± 0.5 cm from 149a	+++	++	39	21.7	1.57		20.6
SOU 01-151a1*	4	Vein, > 8 cm wide, 4 m long	−	tr	88	21.4	3.39		23.5
SOU 01-151a2*	4	Vein, > 8 cm wide, 4 m long, 100% calcite zone	−	−	100	21.7	3.67		
SOU 01-150*	4	Metamorphic Albian (II)	+++	++	39	21.5	1.53		20.2
SOU 01-155*	5	Vein, > 7 cm wide, 1 m long, folded	−	tr	99	21.9	2.71		
SOU 01-154*	5	Metamorphic Albian (II)	+++	+	43	22.5	1.68		
SOU 01-156a*	6	Vein, 2 cm wide, 2 m long,	−	+	93	21.9	2.64		23.1
SOU 01-156b*	6	Metamorphic Albian (II), 1.5 ± 0.5 cm from 156a	++	++	42	22.2	1.19		21.1
SOU 01-160a3*	7	Vein, 1–3 cm wide, 1 m long, 1.2 cm from contact	tr	tr	53	20.6	−3.86		21.8
SOU 01-160a2*	7	Vein, 1–3 cm wide, 1 m long, 0.8 cm from contact	tr	tr	35	20.7	−2.99	0.70830	22.8
SOU 01-160a1*	7	Vein, 1–3 cm wide, 1 m long, 0.3 cm from contact	tr	tr	36	20.8	−2.87		23.0
SOU 01-160b1*	7	Metamorphic Albian (II), 0.35 ± 0.15 cm from contact	+++	++	2.8	21.6	−5.93		19.8
SOU 01-160b2*	7	Metamorphic Albian (II), 0.75 ± 0.15 cm from contact	+++	++	5.0	21.5	−5.85	0.70985	
SOU 01-160b3*	7	Metamorphic Albian (II), 1.15 ± 0.15 cm from contact	+++	++	8.8	21.4	−5.66	0.70958	20.3
SOU 01-160b4*	7	Metamorphic Albian (II), 1.65 ± 0.3 cm from contact	+++	++	11.6	21.2	−5.64		19.9
SOU 01-160b5*	7	Metamorphic Albian (II), 2.15 ± 0.15 cm from contact	+++	++	12.1	21.3	−5.61		
SOU 01-160b6*	7	Metamorphic Albian (II), 2.65 ± 0.3 cm from contact	+++	++	12.9	21.2	−5.63		
SOU 01-160b7*	7	Metamorphic Albian (II), 3.15 ± 0.15 cm from contact	+++	++	13.0	21.2	−5.67		
SOU 01-160b8*	7	Metamorphic Albian (II), 3.65 ± 0.3 cm from contact	+++	++	13.1	21.3	−5.61	0.70944	20.2
SOU 01-160b9*	7	Metamorphic Albian (II), 4.1 ± 0.1 cm from contact	+++	++	12.5	21.4	−5.58		
SOU 01-163a*	7	Vein, 2 cm wide	−	tr	33	20.7	−2.72		22.8
SOU 01-163b*	7	Metamorphic Albian (II), 1.2 ± 0.3 cm from 163a	++	+++	14	21.2	−5.65		20.0
SOU 01-164	8	Metamorphic Albian (II)	+++	+++	34	22.4	−0.99		
VIR 01-129	1	Metamorphic Albian (II)	−	+++	38	21.7	−1.74		
VIR 01-133b	2	Metamorphic Albian (II)			10	21.2	−4.58		
VIR 01-137a*	6	Vein, 2 cm wide, 2 m long,	+	tr	77	21.3	−4.09	0.70854	23.3

Table 1 (*Continued*)

Sample	Location	Type	Mineralogy		Calcite				Silicate
			Biotite	Opaques	wt%	$\delta^{18}O$‰	$\delta^{13}C$‰	$^{87}Sr/^{86}Sr$	$\delta^{18}O$‰
VIR 01-137b*	6	Metamorphic Albian (II), 1.5 ± 0.5 cm from 137a	+++	+++	6.4	23.0	−4.92	0.70977	21.4
VIR 01-139a*	7	Vein, 3 cm wide			94	21.6	−0.16		22.8
VIR 01-139b*	7	Metamorphic Albian (II), 1 ± 0.5 cm from 139a			35	22.0	−4.18		20.9
BOUZ 00-82	1	Metamorphic Albian (III)	+	+++	12	22.4	−3.13		
BOUZ 00-83	1	Metamorphic Albian (III)	+++	+++	11	21.5	−5.63		
BOUZ 01-141a*	2	Vein, 0.5 cm wide	−	−	82	23.7	2.85	0.70735	
BOUZ 01-141b*	2	Metamorphic Albian (II), 1.5 cm from 141a	−	+	47	24.0	1.74	0.70739	
BOUZ 01-144a*	3	Vein, 1.5 cm wide			89	21.0	2.58		
BOUZ 01-144b*	3	Metamorphic Albian (III), 1.5 cm from 144a			31	21.3	0.51		
TAU 01-79a*	6	Vein, 1 cm wide, 1 m long	−	−	88	24.6	1.79		
TAU 01-79b*	6	Metamorphic Albian (II)	−	+	81	24.6	1.80		
TAU 01-80a*	7	Vein, 1 cm wide	−	tr	83	24.7	3.29		
TAU 01-80b*	7	Metamorphic Albian (II)	−	+	72	25.0	2.93		
TAU 01-81a*	8	Vein, 2 cm wide	−	−	90	24.2	3.88	0.70734	
TAU 01-81b*	8	Metamorphic Albian (II)	tr	++	71	24.1	2.35	0.70741	

Samples quoted with an asterisk are associated as vein – host rock pairs. Roman numbers in the *Type* column relate to the metamorphic grade as labelled in Fig. 1b. Symbols for abundance of Bt and opaque minerals are:−: 0%; tr: 0–1%; +: 1–5%; ++: 5–10%; +++: 10–15%. $\delta^{18}O$ values are presented relative to SMOW, $\delta^{13}C$ relative to PDB standards, respectively.

the reactants: if the protolith contains very little calcite, the decarbonation reaction cannot proceed far because of the rapid disappearance of calcite; if the protolith contains very large amounts of calcite, decarbonation is also limited (for example, marbles are the isochemical recrystallization product of limestones). In Fig. 2, we can infer that the calcite/silicate ratio is quite variable, which is the cause of variable decarbonation reaction progress. Goujou et al.
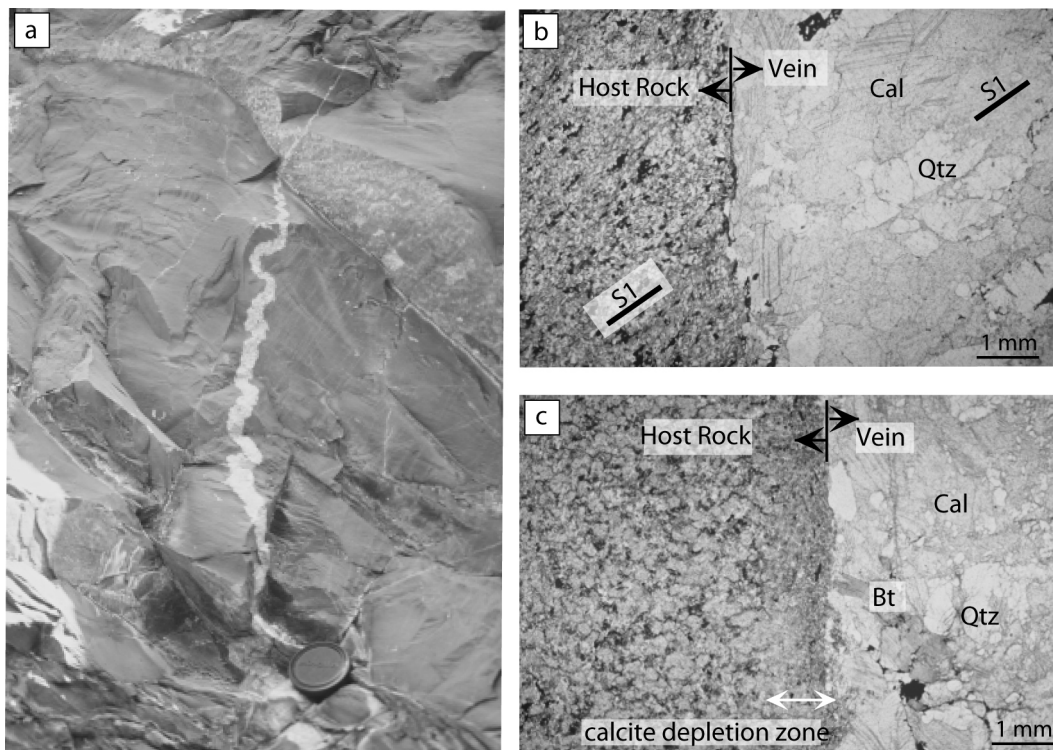

Fig. 3. (**a**) Folded vein crosscutting an Albian calcite-rich black shale where foliation is poorly defined (sample DSX 00-51). (**b**) (**c**) Microscopic views of vein – host rock contacts. In (**b**), foliation S1 is oblique to the contact but define a single orientation on each side. In (**c**), a narrow calcite depletion zone is visible in the host rock close to the vein.
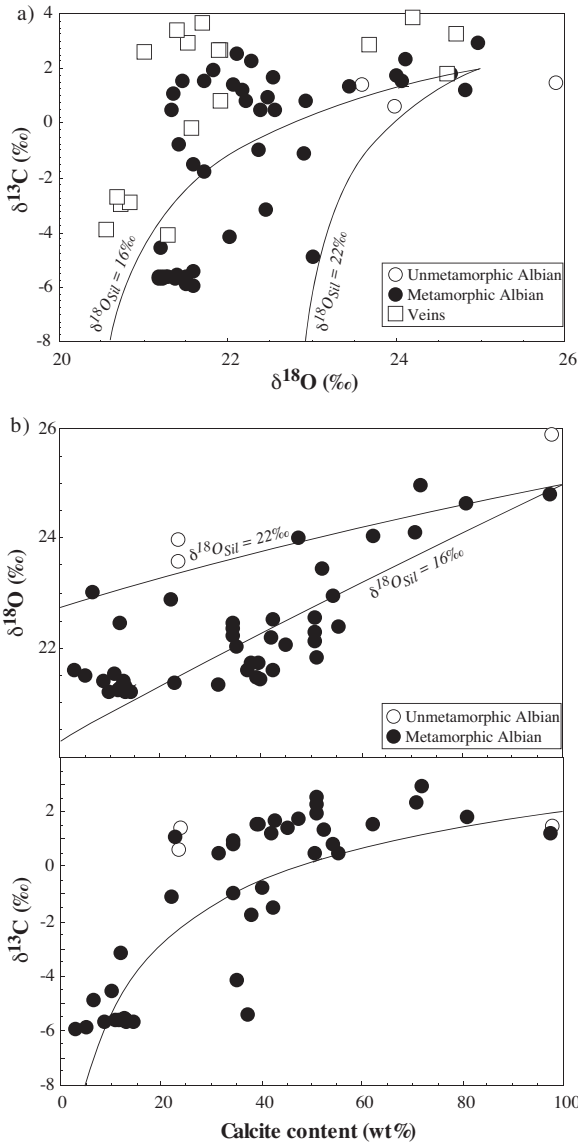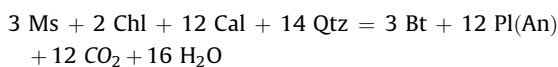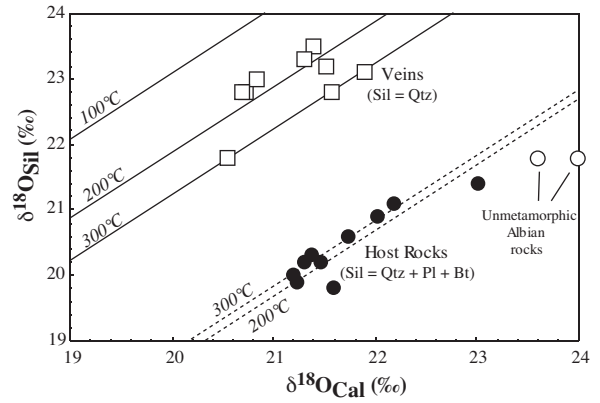
Fig. 5. δ–δ diagram of calcite and silicate phases in veins (squares) and Albian host rocks (circles). Oblique lines represent equilibrium fractionation between minerals calculated after the coefficients of Zheng (1993a,b). See text for details.

these isotopes and acquires lower and lower $\delta^{18}O$ and $\delta^{13}C$ values as decarbonation proceeds. Minimum values are obtained in rocks, which have undergone the most decarbonation, i.e. the rocks with low contents of calcite. This theoretical evolution is described by the curves in Figs. 4a and b. These calculations include the isotopic effects of O equilibration between calcite and a silicate
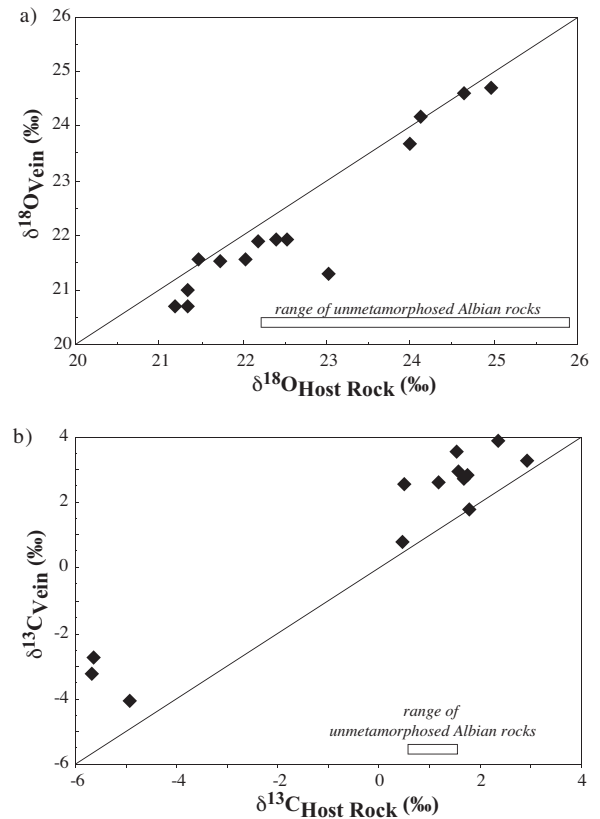

Fig. 4. Stable isotope diagrams for the calcite fraction of Albian rocks and veins. (**a**) Data are compared with theoretical equilibration–decarbonation–dehydration curves (using a Rayleigh-type distillation) where the effects of both decarbonation + dehydration and equilibration between calcite and silicate are taken into account. Two silicate end-members compositions are used in the calculation, 16 and 22‰. The calcite initial compositions are $\delta^{18}O = 25‰$, $\delta^{13}C = 2‰$. (**b**) Oxygen and carbon isotope compositions of Albian rocks reported as a function of their calcite content. Also reported are the theoretical curves of equilibration–decarbonation–dehydration.

(1988) proposed a reaction of dehydration–decarbonation for calcareous siltstones in the area, which leads to biotite and anorthite formation, at about 350 °C:

$$3\ Ms + 2\ Chl + 12\ Cal + 14\ Qtz = 3\ Bt + 12\ Pl(An)$$
$$+ 12\ CO_2 + 16\ H_2O$$

The liberated CO_2 is enriched in both ^{18}O and ^{13}C (Valley, 1986). The remaining calcite is thus depleted in

Fig. 6. Comparison between oxygen (**a**) and carbon (**b**) isotope compositions of the calcite fraction of veins and host rocks. See text for details about calculations.
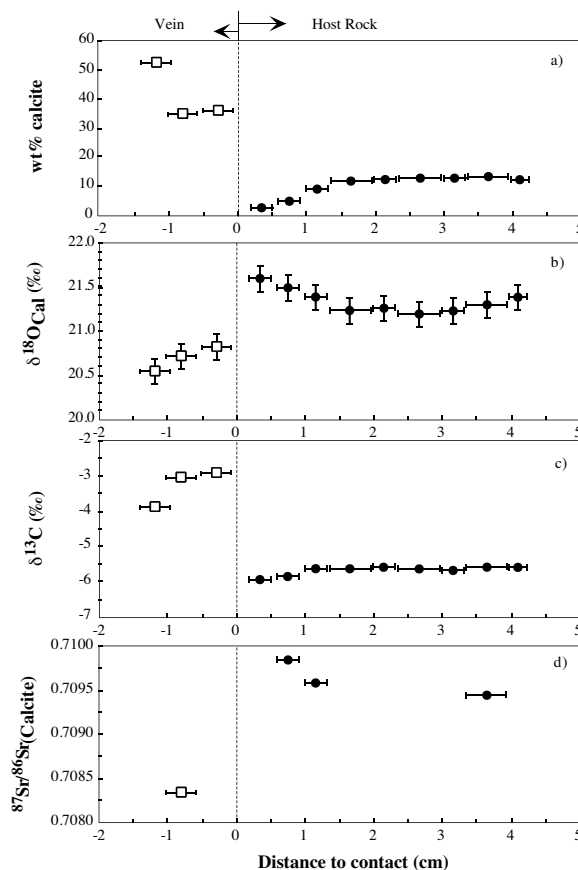
Fig. 7. Evolution of the (**a**) calcite content and (**b**) oxygen, (**c**) carbon and (**d**) strontium isotope compositions along a profile perpendicular to the contact between a vein and its host rock (samples SOU 01-160). Horizontal error bars correspond to the actual width of samples (got by sawing); vertical error bars correspond to the analytical precision. This precision is comprised inside the markers in (**a**), (**c**), and (**d**).

phase. The $\delta^{18}O$ value of the clastic material is set between 22‰ and 16‰ to take account of heterogeneity in clastics between a high-$\delta^{18}O$ clay-rich end-member and a low-$\delta^{18}O$ Qtz-rich one. This range encompasses the value of 21.8‰, actually measured for two Albian unmetamorphic rocks (Table 1). The curves were calculated considering an escaping fluid with H_2O–CO_2 in equal proportions and using the carbon Cal–CO_2 and oxygen Cal–CO_2 and Cal–H_2O fractionations factors of Chacko et al. (1991) and Zheng (1999), respectively, at a temperature of 350 °C. In the calculation of this equilibration–decarbonation–dehydration process, a mole of calcite reacts with a mole of silicate. The results have been transformed into weight % for clarity. In Fig. 4, one can observe that a process of equilibration–decarbonation reproduces rather well the isotopic characteristics of the Albian metamorphic rocks.

Now, considering the quartz – calcite veins, these also display large variations in both $\delta^{18}O$ and $\delta^{13}C$, defining an envelope that is close to that defined by Albian metamorphic rocks, slightly displaced toward higher $\delta^{13}C$ and lower $\delta^{18}O$ values (Fig. 4a). In Fig. 6, in which vein – host rock pairs are considered, we can observe a good correlation between the O and C isotope compositions of the veins and those of the local host rocks. We infer that the isotopic

heterogeneities of the Albian metamorphic rocks are transmitted to the veins, which is a strong argument in favour of a closed system evolution. The studied veins do not require any contribution of externally-derived fluids in the Boucheville Basin. The Sr isotope composition of the Albian metamorphic rocks are consistent with such a model as they can be simply explained by resulting from the mixing of two components (marine carbonate and a detrital clay-rich component) with distinct Sr content and Sr isotope compositions (Fig. 8).

6.2. Mode of vein formation

Veins are composed of calcite and quartz, the abundance of calcite being related to the abundance of calcite in the host rock. In veins, calcite and quartz are in mutual isotopic equilibrium at apparent temperatures (200 °C–300 °C; Fig. 5) lower than those estimated using Raman spectroscopy (530 °C–580 °C; Clerc et al., 2015; Chelalou et al., this issue). This observation may indicate either that veins formed early in the metamorphic history of the Boucheville Basin (recording prograde equilibrium) or that the isotopic equilibration is retrograde; in this latter case the estimated temperature is consistently lower than the

actual measurements near (Chelalou et al., this issue). Regardless of the exact cause of the rather low apparent temperature of equilibrium, the isotopic characteristics of veins argue for their formation at metamorphic conditions.

Veins contain higher amounts of calcite than their host rocks as shown for example by sample SOU 01-160 (Fig. 7a). Interestingly, the amount of calcite in the host decreases near the contact. This can be interpreted as a depletion metasomatic halo around the vein, in which host rock calcite was dissolved, then reprecipitated in the vein. In this example, both the depletion halo and the vein are 2 cm wide. The host rock has lost about half of its initial 13 wt% Cal. Considering a vein 1 m long, 1 m high and 2 cm wide, we can estimate that it contains about 21 kg of calcite using densities of calcite and quartz of 2.71 and 2.66 gm·cm^{-3}, respectively. If we assume that the depletion halo is uniform around the vein and if the initial content of calcite in the host rock does not vary (which is clearly not the case as many samples contain usually 50% of calcite), the total amount of calcite provided by the host rock would be about 7 kg. This crude estimate is a minimum and we thus conclude that the material used in crystal growth in veins originates at least in part from the local host rock, the complementary material being likely derived from underlying volumes of metamorphosed rocks. This is consistent with the isotopic data that imply a fluid regime evolution under closed-system conditions.

The Sr isotope compositions of the Albian rocks and veins also argue for a derivation of the vein material from the local host rock. For two of the four vein–host rock pairs analysed (samples BOUZ 01-141 and TAU 01-81), the $^{87}Sr/^{86}Sr$ ratio is nearly identical ($^{87}Sr/^{86}Sr = 0.70737 \pm 0.0004$; Table 1, Fig. 8). No radiogenic Sr has been incorporated in the calcite phase since crystallization and no input of radiogenic Sr accompanied calcite precipitation. For the two other pairs (VIR 01-137, SOU 01-160), the Sr isotope ratio of the vein is lower than the one of the host rock (Table 1, Fig. 8). In Fig. 7d, the $^{87}Sr/^{86}Sr$ ratio of samples SOU 01-160b increases towards the vein. This is incompatible with an isotopic exchange between Sr of the

Albian rock and Sr from the vein material as the latter has lower $^{87}Sr/^{86}Sr$. We argue that the difference between veins and hosts are related to mode effects. The two samples SOU 01-160b and VIR 01-137b are biotite-rich (Table 1). This mineral formed by recrystallization of clays including sericite during metamorphism – see the equation of Goujou et al. (1988) recalled above. K-rich sericite has a high Rb/Sr ratio and consequently is characterized by an increase of its $^{87}Sr/^{86}Sr$ with time. During metamorphic recrystallization, isotopic equilibrium between unradiogenic Sr from calcite and radiogenic Sr from sericite and biotite is facilitated by ^{87}Sr diffusion through the fluid phase and recrystallization. At the time of vein formation, Cal veins freeze their $^{87}Sr/^{86}Sr$ ratio whereas calcite in the host rock maintains its isotopic equilibrium with the whole rock through ^{87}Sr exchange with Bt. The rate of $^{87}Sr/^{86}Sr$ increase in Cal host rock is even faster after vein formation because the amount of Cal is decreased in the host. This model of closed-system Sr isotope evolution, consistent with the information obtained from stable isotopes, is summarized in Fig. 9.

6.3. Consequences for heat transfer in the Boucheville Basin

The peculiar geometry of the NPMZ along the NPF (Fig. 1) and the observation of some hydraulic fracturing have led Dauteuil and Ricou (1989) to propose that the circulation of hot fluids might have transported the heat necessary to induce metamorphic recrystallization. If heat was advected by fluids locally, the results presented here rule out a regional role of fluids in transporting heat, especially in the Boucheville Basin, and most probably in other neighbouring Albian basins. It is irrefutable that fluids circulated throughout these basins, as recorded by the presence of the quartz – calcite veins described here. These fluids have been generated during metamorphism of Albian rocks through dehydration–decarbonation reactions, and must have escaped from the basins. Given the heterogeneity of the sedimentary assemblage (Fig. 2) and without a precise estimate of the lithological assemblage (what could be done from the work of Chelalou et al., this issue), it would be hazardous to quantify the amount of fluids liberated. It remains that the clay-rich sediments of the Boucheville Basin must have liberated large amounts of H_2O–CO_2 fluids during prograde metamorphism in the
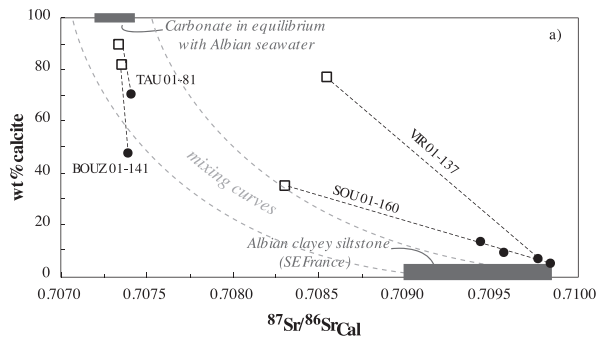

Fig. 8. Relationship between the calcite content and the Sr isotope composition of veins (empty squares) and their local host rocks (HR, black dots). The dashed straight lines link veins-HR pairs. The curvature of the qualitative mixing curves was obtained considering a higher Sr content in calcite than in the clastic material in the original sediment. The field of Albian black shales is from Rousset et al. (2005), the field of carbonate is from Veizer et al. (1999) and encompasses the reference value of 0.7074 from Veizer (1989).
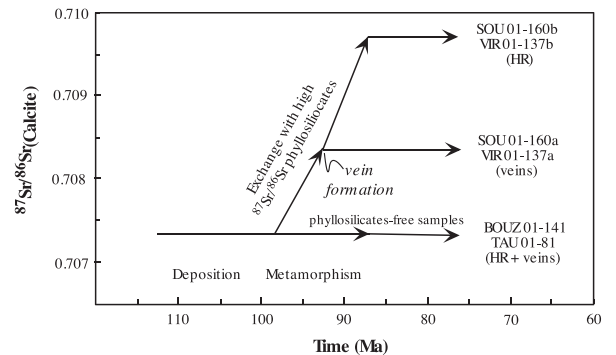

Fig. 9. Model of strontium isotope evolution of the calcitic part of Albian rocks (HR) and veins during sedimentation and metamorphism. An age compilation of the events is available in the Fig. 3 of Clerc et al. (2015).

order of, at strict minimum, 2 kg to 3 kg of fluids per 100 kg of rocks. We can thus propose a hypothesis about the thermal impact of the fluid circulation proposed here. The Albian rocks have been heated from below because of mantle exhumation beneath the Boucheville Basin (Clerc et al., 2015). The first Albian rocks to dehydrate–decarbonate are those at the base of the basin. These reactions led to the origin of fluids that have migrated upwards throughout the basin, advecting heat to higher levels. So, whereas decarbonation–dehydration reaction at the base of the basin may have buffered heat propagation, the flux of fluids upwards might have transported heat. The expected consequence is a relatively homogeneous temperature distribution within the basins, whereas isotherms would have been compressed towards the base of the basin. The Raman spectroscopic data of Chelalou et al. (this issue) consistently emphasize a homogeneous distribution of temperature within the basin, between 530 °C and 580 °C. Thus, if fluid circulation was not the cause of heat transport at the origin of the North Pyrenean Metamorphism, fluid circulation throughout the Albian Basins may have played a significant role in homogenising the temperature field at the scale of the basins.

7. Conclusion

The isotopic analysis of the quartz-calcareous Albian black shales, metamorphosed during the North Pyrenean Metamorphism, in the French Pyrenees, and the associated syn-tectonic veins network suggest the following conclusions.

1/Veins composed of calcite and quartz were formed during the NPM. Host rocks exert a control on the mineralogy of the veins. A significant portion of the elements contributing to calcite growth in veins came from the local host rocks.

2/Veins do not record any infiltration of externally derived fluids as their oxygen and carbon isotope compositions are controlled by those of the local host rocks, in a rock-dominated fluid-rock interaction system.

3/Veins represent the escape pathway of fluids generated during metamorphism through dehydration–decarbonation reaction of the Albian rocks. Metamorphism is a cause, not a consequence, of fluid circulation.

4/Fluids generated within the Boucheville Basin may have acted to homogenize the temperature field in the basin.

Acknowledgements

References

Albarède, F., Michard-Vitrac, A., 1978. Age and significance of the North Pyrenean metamorphism. Earth Planet. Sci. Lett. 40, 327–332.

Boulvais, P., de Parseval, P., D'Hulst, A., Paris, P., 2006. Carbonate alteration associated with talc-chlorite mineralization in the eastern Pyrenees, with emphasis on the St. Barthelemy Massif. Mineralogy and Petrology 88, 499–526.

Boulvais, P., Ruffet, G., Cornichet, J., Mermet, M., 2007. Cretaceous albitization and dequartzification of Hercynian peraluminous granite in the Salvezines Massif (French Pyrénées). Lithos 93, 89–106.

Chacko, T., Mayeda, T.K., Clayton, R.N., Goldsmith, J.R., 1991. Oxygen and carbon isotope fractionations between CO_2 and calcite. Geochim. Cosmochim. Acta 55, 2867–2882.

Chelalou, R., Nalpas, T., Prevost, M., Lahfid, A., Ringenbach, J.-C., Ballard, J.-F., Lagabrielle, Y., 2015. New sedimentological, structural and thermal data on Boucheville Basin. (this issue).

Choukroune, P., 1976. Structure et évolution tectonique de la zone nord-pyrénéenne. Analyse de la déformation dans une portion de chaîne à schistosité sub-verticale. Mem. Soc. geol. France Tome XV (127), 1–116.

Choukroune, P., 1992. Tectonic evolution of the Pyrenees. Annu. Rev. Earth Planet. Sci. 20, 143–158.

Choukroune, P., Le Pichon, X., Séguret, M., Sibuet, J.-C., 1973. Bay of Biscay and Pyrenees. Earth Planet. Sci. Lett. 18, 109–118.

Clerc, C., Lagabrielle, Y., 2014. Thermal control on the modes of crustal thinning leading to mantle exhumation. Insights from the Cretaceous Pyrenean hot paleomargins. Tectonics 33, 1340–1359.

Clerc, C., Boulvais, P., Lagabrielle, Y., de Saint Blanquat, M., 2014. Ophicalcites from the Northern Pyrenean Belt: a field, petrographic and stable isotope study. Int. J. Earth Sci. 103, 141–163.

Clerc, C., Lahfid, A., Monié, P., Lagabrielle, Y., Chopin, C., Poujol, M., Boulvais, P., Ringenbach, J.-C., Masini, E., de St Blanquat, M., 2015. High-temperature metamorphism during extreme thinning of the continental crust: a reappraisal of the North Pyrenean paleo-passive margin. Solid Earth Discuss. 7, 797–857.

Clayton, R.N., Mayeda, T.K., 1963. The use of bromine pentafluorine in the extraction of oxygen from oxides and silicates for isotopic analysis. Geochim. Cosmochim. Acta 27, 43–52.

Dauteuil, O., Ricou, L.-E., 1989. Une circulation de fluides de haute-température à l'origine du métamorphisme crétacé nord-pyrénéen. Geodin. Acta 3, 237–250.

Fabriès, J., Lorand, J.-P., Bodinier, J.-L., 1998. Petrogenetic evolution of orogenic lherzolite massifs in the central and western Pyrenees. Tectonophysics 292, 145–167.

Fallourd, S., Poujol, M., Boulvais, P., Paquette, J.-L., de Saint Blanquat, M., Remy, P., 2014. In situ LA-ICP-MS U–Pb titanite dating of Na–Ca metasomatism in orogenic belts: the North Pyrenean example. Int. J. Earth Sci. 103, 667–682.

Golberg, J.-M., Maluski, H., 1988. Données nouvelles et mise au point sur l'âge du métamorphisme pyrénéen. C. R. Acad. Sci. Paris, Ser. II 306, 429–435.

Golberg, J.-M., Leyreloup, A.F., 1990. High temperature - low pressure Cretaceous metamorphism related to crustal thining (Eastern North Pyrenean Zone, France). Contrib. Mineral. Petrol. 104, 194–207.

Goujou, J.-C., Golberg, J.-M., Leyreloup, A., 1988. Réactions de décarbonatation dans les roches calcaréo-pélitiques de la Ballongue (zone nord-pyrénéenne). 1. Formation de biotite et de plagioclase. C. R. Acad. Sci. Paris, Ser. II 307, 39–44.

Grötsch, J., Billing, I., Vahrenkamp, V., 1998. Carbon-isotope stratigraphy in shallow-water carbonates, implications for Cretaceous black-shale deposition. Sedimentology 45, 623–634.

Henry, P., Azambre, B., Montigny, R., Rossy, M., Stevenson, R.K., 1998. Late mantle evolution of the Pyrenean sub-continental lithospheric mantle in the light of new ^{40}Ar–^{39}Ar and Sm-Nd ages on pyroxenites and peridotites (Pyrenees, France). Tectonophysics 296, 103–123.

McCrea, J.M., 1950. On the isotope chemistry of carbonates and a paleo-temperature scale. J. Chem. Phys. 18, 849–857.

Moine, B., Fortuné, J.P., Moreau, P., Viguier, F., 1989. Comparative mineralogy, geochemistry and conditions of formation of two metasomatic talc and chlorite deposits: Trimouns (Pyrénées, France) and Rabenwald (Eastern Alps, Austria). Economic Geology 84, 1398–1416.

Monchoux, P., 1970. Les lherzolites pyrénéennes, contribution à l'étude de leur minéralogie, de leur genèse et de leurs transformations. Université Paul Sabatier, Toulouse, France (Thesis).

Montigny, R., Azambre, B., Rossy, M., Thuizat, R., 1986. K–Ar study of Cretaceous magmatism and metamorphism in the Pyrenees, age and length of rotation of the Iberian Peninsula. Tectonophysics 129, 257–273.

Nederbragta, A.J., Erlichb, R.N., Fouke1, B.W., Ganssena, G.M., 1998. Palaeoecology of the biserial planktonic foraminifer Heterohelix moremani (Cushman) in the Late Albian to Middle Turonian Circum-North Atlantic. Paleogeogr. Paleoclimatol. Paleoecol. 144, 115–133.

Olivet, J.-L., 1996. La cinématique de la plaque ibérique. Bull. Cent. Rech. Expl. -Prod., Elf Aquitaine 20, 131–195.

Poujol, M., Boulvais, P., Kosler, J., 2010. In-situ LA–ICP–MS U–Th–Pb dating of metasomatic fluid circulation: Evidence of regional-scale albitization in the Pyrenees. J. Geol. Soc. 167, 751–767.

Ravier, J., 1959. Le métamorphisme des terrains secondaires de Pyrénées. Mem. Soc. geol. France Tome XXXVIII (86) (250 p).

Roure, F., Choukroune, P., Berastegui, X., Munoz, J.A., Villien, A., Matheron, P., Bareyt, M., Séguret, M., Camara, P., Deramond, J., 1989. ECORS deep seismic data and balanced cross sections: gemetric constraints on the evolution of the Pyrenees. Tectonics 8, 41–50.

Rousset, D., Lancelot, J., Verdoux, P., Clauer, N., Leclerc, S., 2005. Influence of local fluid flow on properties of low permeability Cretaceous siltstones (South-Eastern France): implications for nuclear waste deep repository. J. Geochem. Explor. 87, 1–18.

Schärer, U., de Parseval, P., Polvé, M., de Saint Blanquat, M., 1999. Formation of the Trimouns talc-chlorite deposit (Pyrenees) from persistent hydrothermal activity between 112 and 97 Ma. Terra Nova 11, 30–37.

Souquet, P., Debroas, E.-J., Boirie, J.-M., Pons, P., Fixari, G., Dol, J., Thieuloy, J.-P., Bonnemaison, M., Manivit, H., Peybernès, B., 1985. Le groupe du Flysch noir (Albocénomanien) dans les Pyrénées. Bull. Cent. Rech. Expl. Elf Aquitaine 9, 183–252.

Valley, J.W., 1986. Stable isotope geochemistry of metamorphic rocks. In: Valley, J.W., Taylor, Jr., H.P., O'Neil, J.R. (Eds.), Stable Isotopes in High Temperature Geological Processes. Reviews in Mineralogy, Vol. 16, Mineralogical Society of America, pp. 445–489.

Veizer, J., 1989. Strontium isotopes in seawater through time. Annu. Rev. Earth Planet. Sci. 17, 141–167.

Veizer, J., Ala, D., Azmy, K., Bruckschen, P., Buhl, D., Bruhn, F., Carden, G.A.F., Diener, A., Ebneth, S., Godderis, Y., Jasper, T., Korte, C., Pawallek, F., Podlaha, O.G., Strauss, H., 1999. $^{87}Sr/^{86}Sr$, $\delta^{13}C$ and $\delta^{18}O$ evolution of Phanerozoic seawater. Chem. Geol. 161, 59–88.

Weissert, H., Bréhéret, J.-G., 1991. A carbonate carbon-isotope record from Aptian-Albian sediments of the Vocontian trough (SE France). Bull. Soc. geol. France 162, 1133–1140.

Zheng, Y.F., 1993a. Calculation of oxygen isotope fractionation in anhydrous silicate minerals. Geochim. Cosmochim. Acta 57, 1079–1091.

Zheng, Y.F., 1993b. Calculation of oxygen isotope fractionation in hydroxyl-bearing silicates. Earth Planet. Sci. Lett. 120, 247–263.

Zheng, Y.F., 1999. Oxygen isotope fractionation in carbonate and sulfate minerals. Geochem. J. 33, 109–126.